Published in final edited form as:

Science. 2016 January 22; 351(6271): 379–384. doi:10.1126/science.aad3839.

Oligodendrocyte precursors migrate along vasculature in the developing nervous system

Hui-Hsin Tsai[1,*], **Jianqin Niu**[1,*], **Roeben Munji**[2], **Dimitrios Davalos**[3], **Junlei Chang**[4], **Haijing Zhang**[4,5,6,7], **An-Chi Tien**[1], **Calvin J. Kuo**[4], **Jonah R. Chan**[8], **Richard Daneman**[2], and **Stephen P. J. Fancy**[1,8,9,10,†]

[1]Department of Pediatrics, University of California at San Francisco (UCSF), San Francisco, CA 94158, USA

[2]Departments of Pharmacology and Neuroscience, University of California at San Diego (UCSD), San Diego, CA 92093, USA

[3]Department of Neurosciences, Lerner Research Institute, Cleveland Clinic Foundation, Cleveland, OH 44195, USA

[4]Division of Hematology, Department of Medicine, Stanford University, Stanford, CA 94305, USA

[5]Department of Urology, Cleveland Clinic Foundation, Cleveland, OH 44195, USA

[6]Howard Hughes Medical Institute (HHMI), Chevy Chase, MD 20815, USA

[7]Duke University School of Medicine, Durham, NC 27710, USA

[8]Department of Neurology, UCSF, San Francisco, CA 94158, USA

[9]Division of Neonatology, UCSF, San Francisco, CA 94158, USA

[10]Newborn Brain Research Institute, UCSF, San Francisco, CA 94158, USA

Abstract

Oligodendrocytes myelinate axons in the central nervous system and develop from oligodendrocyte precursor cells (OPCs) that must first migrate extensively during brain and spinal cord development. We show that OPCs require the vasculature as a physical substrate for migration. We observed that OPCs of the embryonic mouse brain and spinal cord, as well as the human cortex, emerge from progenitor domains and associate with the abluminal endothelial surface of nearby blood vessels. Migrating OPCs crawl along and jump between vessels. OPC migration in vivo was disrupted in mice with defective vascular architecture but was normal in mice lacking pericytes. Thus, physical interactions with the vascular endothelium are required for OPC migration. We identify Wnt-Cxcr4 (chemokine receptor 4) signaling in regulation of OPC-

†Corresponding author. stephen.fancy@ucsf.edu.
*These authors contributed equally to this work.

SUPPLEMENTARY MATERIALS
www.sciencemag.org/content/351/6271/379/suppl/DC1
Materials and Methods
Figs. S1 to S18
References (*36–40*)
Movies S1 to S3

endothelial interactions and propose that this signaling coordinates OPC migration with differentiation.

Oligodendrocytes, the myelinating cells of the central nervous system (CNS), support rapid saltatory nerve conduction and maintain axon integrity through metabolic coupling (1, 2). Oligodendrocyte precursor cells (OPCs) arise from the ventricular zone in the embryonic brain and spinal cord, in domains defined through pattern formation (3, 4). From these domains, OPCs migrate widely through the CNS to achieve uniform distribution (fig. S1).

The CNS is built by cells migrating away from their places of origin to construct mature neural tissue. Neuroblasts disperse in radial and tangential patterns (5) following substrates such as radial glial cells (5, 6), corticofugal fibers (7), or Bergmann glia (8). Postnatal neuronal migration is more limited. In the rostral migratory stream, neuroblasts crawl over one another (9) and along blood vessels to get from the subventricular zone to the olfactory bulb (10–12). Astrocytes seem to migrate only radially during development, following radial glia without secondary tangential migration. Thus, astrocytes occupy restricted spatial domains in adulthood related to their embryonic site of origin (13).

Oligodendrocyte precursor cells, which migrate more extensively than neurons and other glia (4), must also recognize their path and migrate through often-compact developing tissue before interactions with their targets halt their migration. OPCs also maintain this capacity in response to demyelination in the adult CNS (14). OPC motility is regulated by cell-intrinsic mechanisms (15, 16), polarity (17), and extracellular cues (18–20). Various substrates have been proposed as putative candidates for OPC migration (21). Here we show that OPCs migrate along the vasculature through the developing CNS and that Wnt signaling regulates these OPC-endothelial interactions.

In the developing mouse forebrain, the first OPCs originate from ventral regions of the medial ganglionic eminence and anterior entopeduncular area at embryonic day 12 (E12) (Fig. 1A) (4). The vascular network is established before OPC emergence (22). At E7.5 to E8.5, a perineural vascular plexus surrounds the ventral neural tube. Angiogenic endothelial sprouts invade the neuro-epithelium from the pial surface to periventricular areas by E11.5, with the blood-brain barrier likely established at this time (22, 23), generating a periventricular vascular plexus (24).

We first assessed the migration of OPCs in the developing mouse brain (see supplementary materials and methods). Migratory OPCs, defined by the expression of platelet-derived growth factor receptor α (PDGFRα), appear at E12 and stream away from the medial ganglionic eminence, in association with this vascular scaffold (Fig. 1B and fig. S2). Many of these migratory OPCs are elongated along blood vessels (Fig. 1C), with their cell bodies directly on the abluminal endothelial surface and a single, long leading process along the vessel (Fig. 1D and *A in fig. S1D). Indeed, 58% (±4.4%) of OPCs have their cell bodies directly on a vessel wall (Fig. 1F), and of the remainder, 67% (±8.9%) display at least one observable process (which can be more than 30 μm in length) that engages a vessel (* in Fig. 1, E and F). By E14, OPCs migrating dorsally reach the subpallial-to-pallial boundary (Fig. 1A and fig. S1B), continuing to show an intimate association with the vasculature (Fig. 1G),

elongated along vessels (Fig. 1H), and often extending one or more processes between vessels (* in Fig. 1I and *B and *C in fig. S1D). The number of OPCs in the mouse cortex increases (4) by a factor of ~3 between E16 and E18. Olig2$^+$ cells migrating from deep to superficial cortical layers palisade along the vasculature that penetrates the cortex at E18 (Fig. 1J and fig. S1C).

A similar association of OPCs with vasculature is seen during development of the human cortex. The first Olig2-expressing cells to arrive in the human outer cortex at gestational week 14 appose penetrating vessels (Fig. 1K); association of Olig2$^+$ and PDGFRα$^+$ OPCs with blood vessels remains evident at gestational weeks 18 and 24 (Fig. 1, L and M). Migrating human OPCs, expressing PDGFRα, are morphologically similar to those of mice in that they extend single leading processes in the direction of movement along and toward vessels (Fig. 1N).

To live-image OPC migration in acute slices of the developing brain, we labeled vessels of *Olig2–green fluorescent protein (GFP)* reporter mice by intracardiac infusion of rhodamine-lectin. We selected brain slices to observe regions with actively migrating OPCs (4), including E16 and E18 cortex. OPCs demonstrate two behaviors during migration on vessels: crawling and jumping. Crawling is characterized by the cell body maintaining contact with the abluminal endothelial surface (Fig. 2A, fig. S3, and movies S1 and S2). Jumping is characterized by the OPC extending a leading process from one vessel toward another, followed by translocation of the cell body to make contact with the new vessel (Fig. 2B and movie S3). Jumping is more rapid than crawling, presumably entailing fewer physical contacts with the endothelial surface. The association of migrating OPCs with the vasculature is not limited to the embryonic brain; it is also found in the spinal cord (Fig. 2, C to H) and at later postnatal times when OPCs are required to migrate (fig. S4).

To study the requirement for OPC migration along a vascular scaffold, we used both conventional and conditional transgenic knockout mice to disrupt vascular development. In mice, the orphan G protein–coupled receptor 124 (GPR124), which is expressed by endothelium and pericytes within the CNS, is essential for developmental vascular sprouting (25) (Fig. 3A). At E11, mice lacking GPR124 exhibit CNS vascular patterning defects and reduced vascularization (25), as well as glomeruloid vascular abnormalities (Fig. 3J) characterized by highly irregular, multilayered endothelial aggregates with peripheral PDGFRβ$^+$ pericyte investment and lack of ventricularly directed endothelial filopodia (25).

We hypothesized that OPC dispersal would be abnormal in E14 *GPR124*$^{-/-}$ embryos. In these mice, Isl1/2-expressing motor neurons, which also derive from the motor neuron precursor (pMN) domain of the spinal cord, migrate in normal numbers to the ventral gray matter (Fig. 3C). Additionally, Glast$^+$ radial glial fibers appear normal (fig. S5A), and brain lipid binding protein (BLBP)–expressing astrocytes, which leave the ventricular zone at the same time as OPCs from domains adjacent to the pMN, migrate normally in spinal cord (Fig. 3D). However, OPCs abnormally accumulated in the pMN and failed to egress normally from the spinal cord ventricular zone (Fig. 3E). Seventy percent fewer OPCs dispersed into the surrounding gray matter (fig. S7A) ($*P = 7.3 \times 10^{-5}$). Rates of OPC cell death were unchanged (fig. S5B), which suggests that the problem is in migration. Because

GPR124 is expressed by both endothelium and pericytes, we used *Cdh5-cre:Gpr124(fl/fl)* mice (Cdh5cre is vascular endothelium–specific VE-Cadherin-cre) to target loss of function to the vascular endothelium (Fig. 3F and fig. S6). We observed the same OPC migration deficit, ruling out a cell-intrinsic effect of Gpr124 loss in OPCs and showing that *GPR124* function in the endothelium is required to regulate OPC migration. Vascular development is also deficient in the brains of E14 GPR124$^{-/-}$ mice, with associated severe OPC migration deficits. OPCs expressing PDGFRα and Olig2 show reductions in migration (Fig. 3, G and H, and fig. S7B), reaching only as far as the limits of the ventral vascular plexus (Fig. 3H), and accumulate in clumps around glomeruloid malformations (Fig. 3K and fig. S7D). In *PDGFR*β-null mice, which lack all pericytes (26), OPC migration was maintained (fig. S8). Thus, OPCs require an endothelial vascular scaffold, but not pericytes, as a physical substrate for migration throughout the developing CNS (Fig. 3I).

Cessation of OPC migration on vasculature and detachment from the endothelium might be coupled to the onset of OPC differentiation, which suggests that negative regulators of OPC terminal differentiation might mediate an interaction between OPCs and the endothelium. The Wnt pathway inhibits OPC differentiation (27–29), leading us to question its role in OPC migration and interaction with the endothelium. We made use of *Olig2-cre:Apc(fl/fl)* mice (28) because they show constitutively active Wnt signaling in OPCs due to the conditional loss of the obligate Wnt repressor *adenomatous polyposis coli* (*APC*). In addition to delays in OPC differentiation in these mice (fig. S9) (28) with resulting hypomyelination, we observed aberrant clusters of OPCs associated with vasculature throughout the brain and spinal cord (Fig. 4, A to D, and fig. S10A) at early post-natal times. OPC aggregation around vessels and absence of increased proliferation (fig. S10B) suggest that Wnt activation in OPCs drives their attraction to the vascular scaffold and that high Wnt tone in OPCs in *Olig2-cre:Apc(fl/fl)* mice leads to an inability to dissociate from the vasculature and disperse normally into CNS parenchyma (fig. S11). A loss of Wnt tone in OPCs, in cortical slice cultures treated with the small-molecule Wnt inhibitor XAV939 (29), results in a 76% ($P = 1.55 \times 10^{-5}$) reduction in OPC recruitment to the microvasculature at postnatal day 1 (P1) and a 71% ($P = 0.0004$) reduction in their migration to the outer cortex (fig. S12). OPCs themselves are a source of the ligands Wnt7a and Wnt7b during their embryonic migration in the brain and spinal cord (Fig. 4E and fig. S13). These ligands act cell-autonomously to activate the Wnt pathway in OPCs at later postnatal times (30), suggesting them as candidates for the source of Wnt mediating the interaction with the endothelium during earlier OPC migration.

To identify how Wnt pathway activation in OPCs promotes their attraction to the endothelium, we analyzed mRNA transcripts up-regulated in mouse Wnt-activated OPCs [from Olig2cre/DA-Cat mice (27, 29), in which Olig2-cre allows conditional expression of floxed dominant-active β-catenin]. One of the most highly up-regulated factors in Wnt-activated OPCs was the chemokine receptor Cxcr4, which is a direct Wnt target in other systems (31) and binds the ligand Sdf1 (Cxcl12), which is expressed by the endothelium throughout OPC developmental migration (Fig. 4H and fig. S14A). Cxcr4 has been implicated in OPC migration (32, 33), but not in connection with the Wnt pathway or the vasculature. We detected up-regulation of *Cxcr4* mRNA in the clustered Wnt-activated OPCs associated with vessels in the brain and spinal cord of *Olig2-cre:Apc(fl/fl)* mice (Fig.

4, F and G). Furthermore, treatment of these mice in vivo with the Cxcr4/Sdf1 antagonist AMD3100 (10) between developmental ages P3 and P10 leads to a reversal of vessel-associated OPC clustering [which is not due to direct AMD3100 effects on OPC differentiation (figs. S15 and S16)] throughout the CNS (Fig. 4, I and J, and fig. S10A, spinal cord; Fig. 4K and fig. S10C, ex vivo corpus callosum), demonstrating a Wnt-activated, Cxcr4-dependent mechanism driving attraction of OPCs to the vascular scaffold. *Cxcr4* is expressed by OPCs during embryonic developmental migration (fig. S14B) but is down-regulated along with Wnt pathway down-regulation in differentiating mature oligodendrocytes (fig. S14, C and D). Furthermore, the loss of *Cxcr4* function leads to a diminished migratory ability of OPCs in the developing CNS (fig. S17). Wnt activation in OPCs therefore mediates their attraction to the vasculature during migration and also blocks their differentiation (27), coupling the timing of these two events, with Wnt down-regulation required for appropriate endothelial dissociation and subsequent differentiation (fig. S18).

Until now, the means by which OPCs negotiate their way through dense CNS tissue and distribute throughout the developing CNS have been unclear. We show that OPCs require a vascular scaffold as a physical substrate for migration. A similar association of OPCs with vasculature in the developing human cortex suggests common modes of migration across mammalian species. We demonstrate a physical interaction that brings migrating OPCs into intimate contact with the endothelium. Wnt pathway activation of Cxcr4 in OPCs mediates their attraction to the endothelium, most likely via the endothelial-expressed Sdf1 ligand (although an alternative cannot be completely excluded), and prevents these cells from differentiating while associated with the vasculature during migration. OPCs are a source of Wnt7a and Wnt7b, and considering that endothelial-expressed Gpr124 is a Wnt7-specific coactivator of canonical Wnt signaling (34, 35), it will be interesting to consider the effects of OPCs on the developing vasculature during their migration.

The mechanisms directing OPC migration during development are likely to be similar, if not identical, to those of the injured or diseased nervous system. OPC migration into demyelinated areas is critical in human diseases (14) such as multiple sclerosis and also in hypoxic injury of the newborn brain. It will be important to establish the contribution of this mode of migration for OPC distribution into areas of injury and to uncover how dysfunction may contribute to disease progression in these debilitating human conditions.

Supplementary Material

Refer to Web version on PubMed Central for supplementary material.

Acknowledgments

We thank D. Rowitch (UCSF) for *Olig2-GFP* mice and comments on the manuscript. Procurements of human brain tissues from the UCSF Pediatric Neuropathology Research Laboratory have been supported by grants from the University of California (142657), the National Institute of Neurological Disorders and Stroke (1P01 NS083513), and HHMI. J.C. is supported by an American Heart Association Postdoctoral Fellowship (15POST23020039). This work was supported by grants from the NIH (1R01NS064517 to C.J.K.) and the National Multiple Sclerosis Society (RG 5216-A-1 to S.P.J.F.) and Race to Erase MS (to S.P.J.F.). The supplementary materials contain additional data.

REFERENCES AND NOTES

1. Fünfschilling U, et al. Nature. 2012; 485:517–521. [PubMed: 22622581]
2. Lee Y, et al. Nature. 2012; 487:443–448. [PubMed: 22801498]
3. Lu QR, et al. Cell. 2002; 109:75–86. [PubMed: 11955448]
4. Kessaris N, et al. Nat Neurosci. 2006; 9:173–179. [PubMed: 16388308]
5. Sidman RL, Rakic P. Brain Res. 1973; 62:1–35. [PubMed: 4203033]
6. Nadarajah B, Brunstrom JE, Grutzendler J, Wong RO, Pearlman AL. Nat Neurosci. 2001; 4:143–150. [PubMed: 11175874]
7. O'Rourke NA, Dailey ME, Smith SJ, McConnell SK. Science. 1992; 258:299–302. [PubMed: 1411527]
8. Komuro H, Rakic P. J Neurosci. 1995; 15:1110–1120. [PubMed: 7869087]
9. Lois C, Alvarez-Buylla A. Science. 1994; 264:1145–1148. [PubMed: 8178174]
10. Kokovay E, et al. Cell Stem Cell. 2010; 7:163–173. [PubMed: 20682445]
11. Snapyan M, et al. J Neurosci. 2009; 29:4172–4188. [PubMed: 19339612]
12. Goldman SA, Chen Z. Nat Neurosci. 2011; 14:1382–1389. [PubMed: 22030549]
13. Tsai HH, et al. Science. 2012; 337:358–362. [PubMed: 22745251]
14. Franklin RJM, ffrench-Constant C. Nat Rev Neurosci. 2008; 9:839–855. [PubMed: 18931697]
15. Finzsch M, Stolt CC, Lommes P, Wegner M. Development. 2008; 135:637–646. [PubMed: 18184726]
16. Binamé F, Sakry D, Dimou L, Jolivel V, Trotter J. J Neurosci. 2013; 33:10858–10874. [PubMed: 23804106]
17. Miyamoto Y, Yamauchi J, Tanoue A. J Neurosci. 2008; 28:8326–8337. [PubMed: 18701695]
18. Tsai HH, Tessier-Lavigne M, Miller RH. Development. 2003; 130:2095–2105. [PubMed: 12668624]
19. Garcion E, Faissner A, ffrench-Constant C. Development. 2001; 128:2485–2496. [PubMed: 11493565]
20. Tsai HH, et al. Cell. 2002; 110:373–383. [PubMed: 12176324]
21. Baron-Van Evercooren A, et al. Glia. 1996; 16:147–164. [PubMed: 8929902]
22. Daneman R, et al. Proc Natl Acad Sci USA. 2009; 106:641–646. [PubMed: 19129494]
23. Stenman JM, et al. Science. 2008; 322:1247–1250. [PubMed: 19023080]
24. Hogan KA, Ambler CA, Chapman DL, Bautch VL. Development. 2004; 131:1503–1513. [PubMed: 14998923]
25. Kuhnert F, et al. Science. 2010; 330:985–989. [PubMed: 21071672]
26. Daneman R, Zhou L, Kebede AA, Barres BA. Nature. 2010; 468:562–566. [PubMed: 20944625]
27. Fancy SP, et al. Genes Dev. 2009; 23:1571–1585. [PubMed: 19515974]
28. Fancy SP, et al. Nat Neurosci. 2014; 17:506–512. [PubMed: 24609463]
29. Fancy SP, et al. Nat Neurosci. 2011; 14:1009–1016. [PubMed: 21706018]
30. Yuen TJ, et al. Cell. 2014; 158:383–396. [PubMed: 25018103]
31. Choe Y, Pleasure SJ. Dev Neurosci. 2012; 34:502–514. [PubMed: 23257686]
32. Banisadr G, et al. Neurobiol Dis. 2011; 44:19–27. [PubMed: 21684336]
33. Dziembowska M, et al. Glia. 2005; 50:258–269. [PubMed: 15756692]
34. Vanhollebeke B, et al. eLife. 2015; 4:e06489.
35. Posokhova E, et al. Cell Rep. 2015; 10:123–130. [PubMed: 25558062]

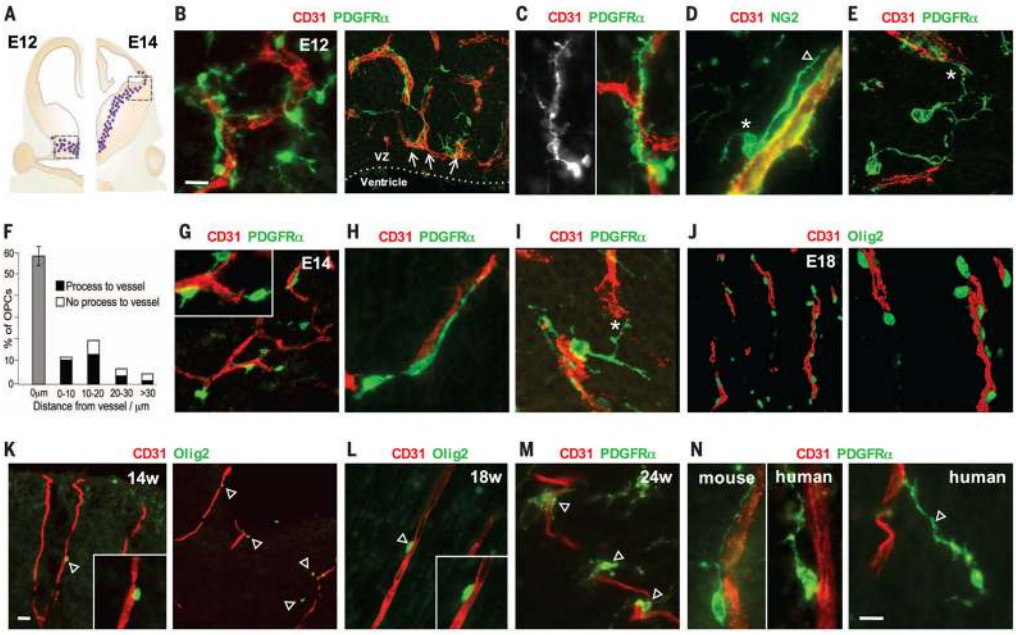

Fig. 1. Association of migratory OPCs with vessels in the developing mouse and human brain

(**A**) OPCs (dots) first appear from the ventral medial ganglionic eminence of the mouse brain at E12 (left) and migrate away from the ventricular zone to reach the subpallial-to-pallial boundary at E14 (right). (**B** to **E**) Images taken from the boxed area on the left side of (A). (B) PDGFRα$^+$ migratory OPCs at E12 associate tightly with CD31$^+$ vasculature and show elongated morphology along vessels (C), often with cell bodies on the endothelial surface [* in (D)], extending a leading process along [arrowhead in (D)] or toward [* in (E)] a vessel. VZ, ventricular zone. (**F**) Quantification of OPC association with vessels at E12 (1056 cells measured, $n = 4$ animals). Error bar indicates SD. (**G** to **I**) Images taken from the boxed area on the right side of (A). Migratory OPCs at the subpallial-to-pallial boundary at E14 maintain tight association with the vasculature (G), with process extension along (H) and between [* in (I)] vessels. Inset in (G) shows zoomed-in view. (**J**) Migrating Olig2$^+$ OPCs in the E18 cortex palisade along cortical penetrating vessels. (**K** to **N**) (K) The first OPCs (Olig2$^+$ and PDGFRα$^+$) to arrive in the developing human outer cortex closely associate with vessels at gestational weeks 14 (14w) (K), 18 (L), and 24 (M) and show similar morphological association with vessels as in mice [left, (N)], with leading processes that can be as long as 65 μm [arrowhead, right (N)]. Scale bars: 10 μm [(B) and (N)]; 20 μm (K).

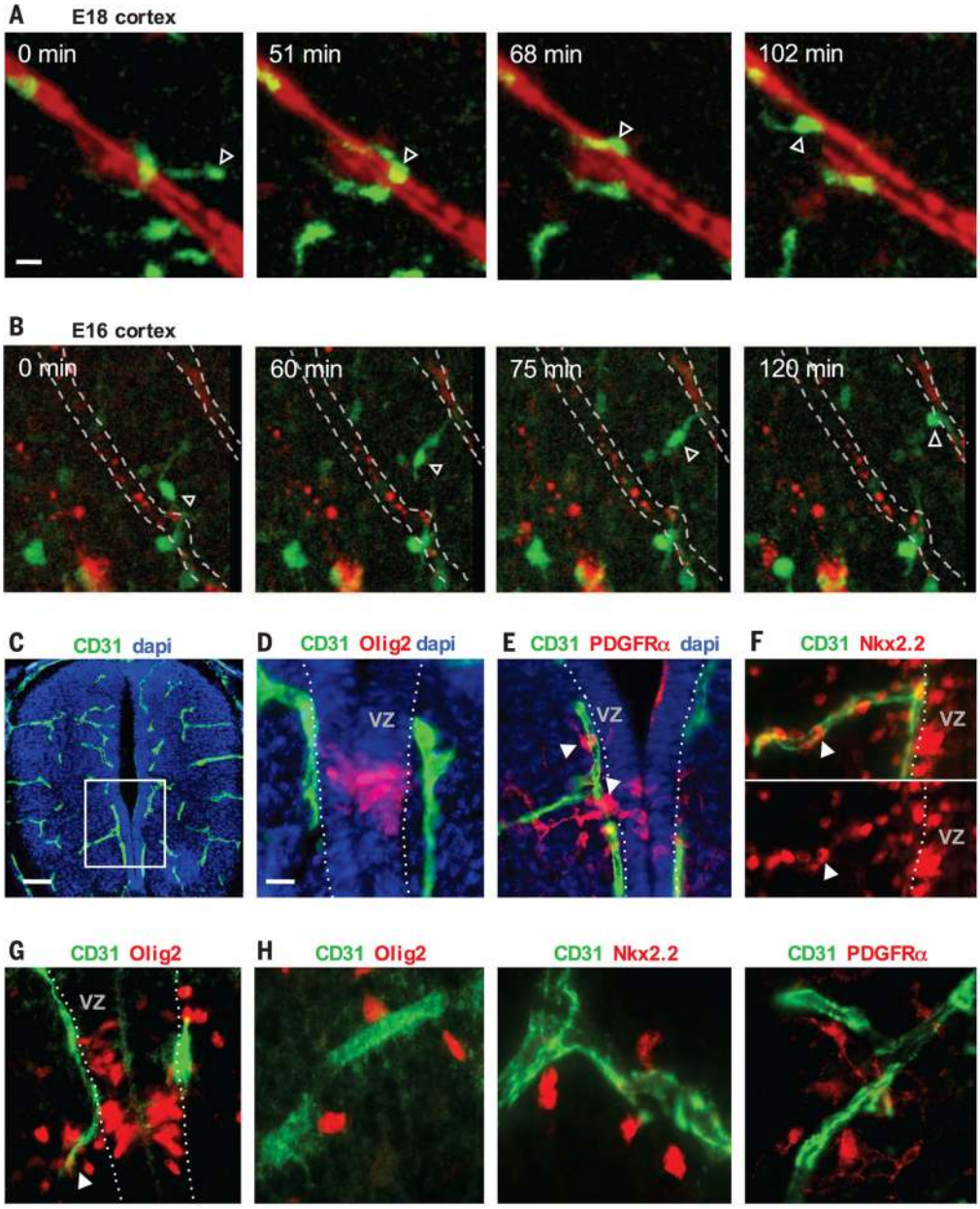

Fig. 2. OPC crawling and jumping directed motility on vessels

(**A** and **B**) Time-lapse imaging in slice cultures of the embryonic *Olig2-GFP* mouse cortex showing GFP expression (green) and vessels (red). (A) A GFP-expressing OPC (arrowhead) crawls along a penetrating vessel in the E18 cortex (movie S1). (B) An OPC in the E16 cortex (arrowhead) (movie S3) demonstrates jumping motility between vessels, extending a process to a parallel cortical penetrating vessel, before movement of the cell body onto the new vessel. (**C** and **D**) Olig2-expressing OPCs define the pMN domain of the spinal cord ventricular zone at E12. (D) shows a zoomed-in view of the boxed area in (C). dapi, 4′,6-diamidino-2-phenylindole. (**E** and **F**) The first PDGFRα- and Nkx2.2-expressing OPCs (arrowheads) emerge from the pMN immediately onto and along the adjacent $CD31^{+}$ vasculature. (**G** and **H**) (G) OPCs tend to leave the pMN at E14 along a vessel that branches

at the pMN (arrowhead), and these cells remain associated with vessels as they continue to disperse throughout the ventral spinal cord (H). Scale bars: 10 μm [(A) and (D)]; 40 μm (C).

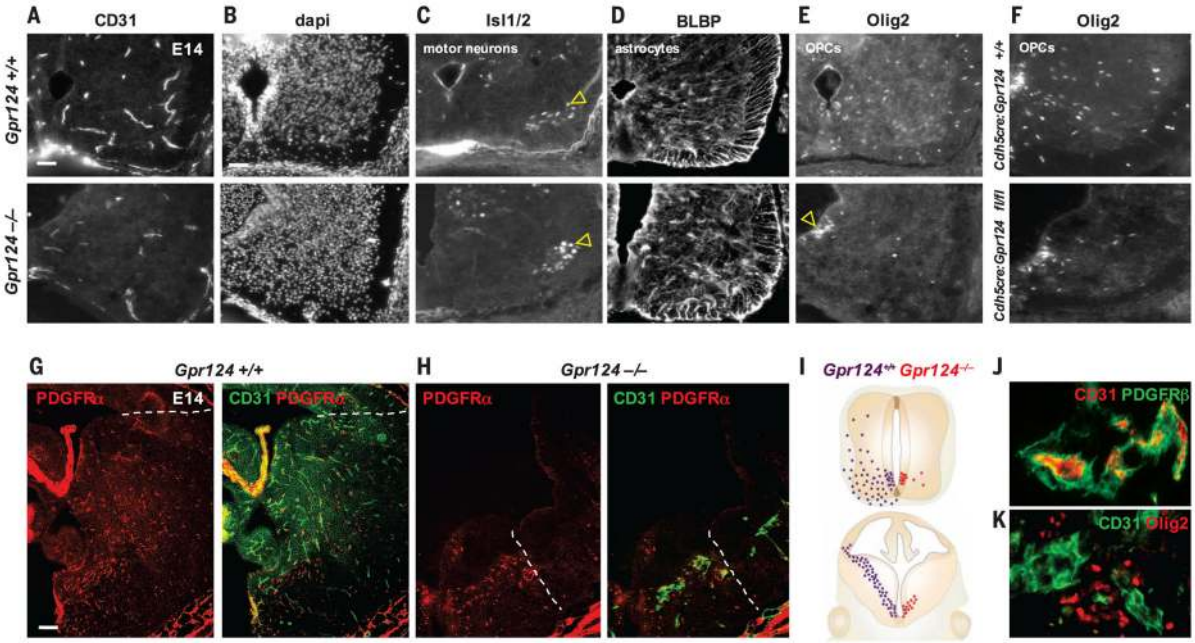

Fig. 3. OPCs require a vascular scaffold for migration

(**A** and **B**) (A) Gpr124$^{-/-}$ embryos exhibit CNS vascular patterning defects at E14, leaving the ventral spinal cord [dapi in (B)] with reduced vascularization compared with controls. (**C**) Islet1/2^{+} motor neurons migrate in normal numbers at E14, from the pMN to ventrolateral gray matter (arrowheads) in Gpr124$^{-/-}$ cords. (**D**) BLBP-expressing astrocytes also migrate normally from ventricular zone domains adjacent to the pMN into the surrounding gray matter in Gpr124$^{-/-}$. (**E** and **F**) (E) OPC (Olig2^{+}) emigration from the ventricular zone is severely disrupted in Gpr124$^{-/-}$ [(E) and (I)] and Cdh5cre/Gpr124-floxed (F) spinal cord with accumulation of OPCs in the pMN [arrowhead in (E)]. (**G**) By E14, OPCs (PDGFRα^{+}) in wild-type (WT) Gpr124$^{+/+}$ brains migrate as far as the subpallial-to-pallial boundary (dotted line). (**H** and **I**) (H) Vascular development (CD31^{+} vessels) is highly truncated in the brains of E14 Gpr124$^{-/-}$ mice, with associated severe OPC migration deficits (I). OPCs migrate only as far as the limits of the ventral vascular plexus [dotted line in (H)]. (**J** and **K**) (J) Absence of Gpr124 leads to vascular abnormalities (glomeruloid malformations) in which OPCs (Olig2^{+}) accumulate in clumps in the E14 Gpr124$^{-/-}$ brain (K). Scale bars: 30 μm [(A) and (B)]; 60 μm (G).

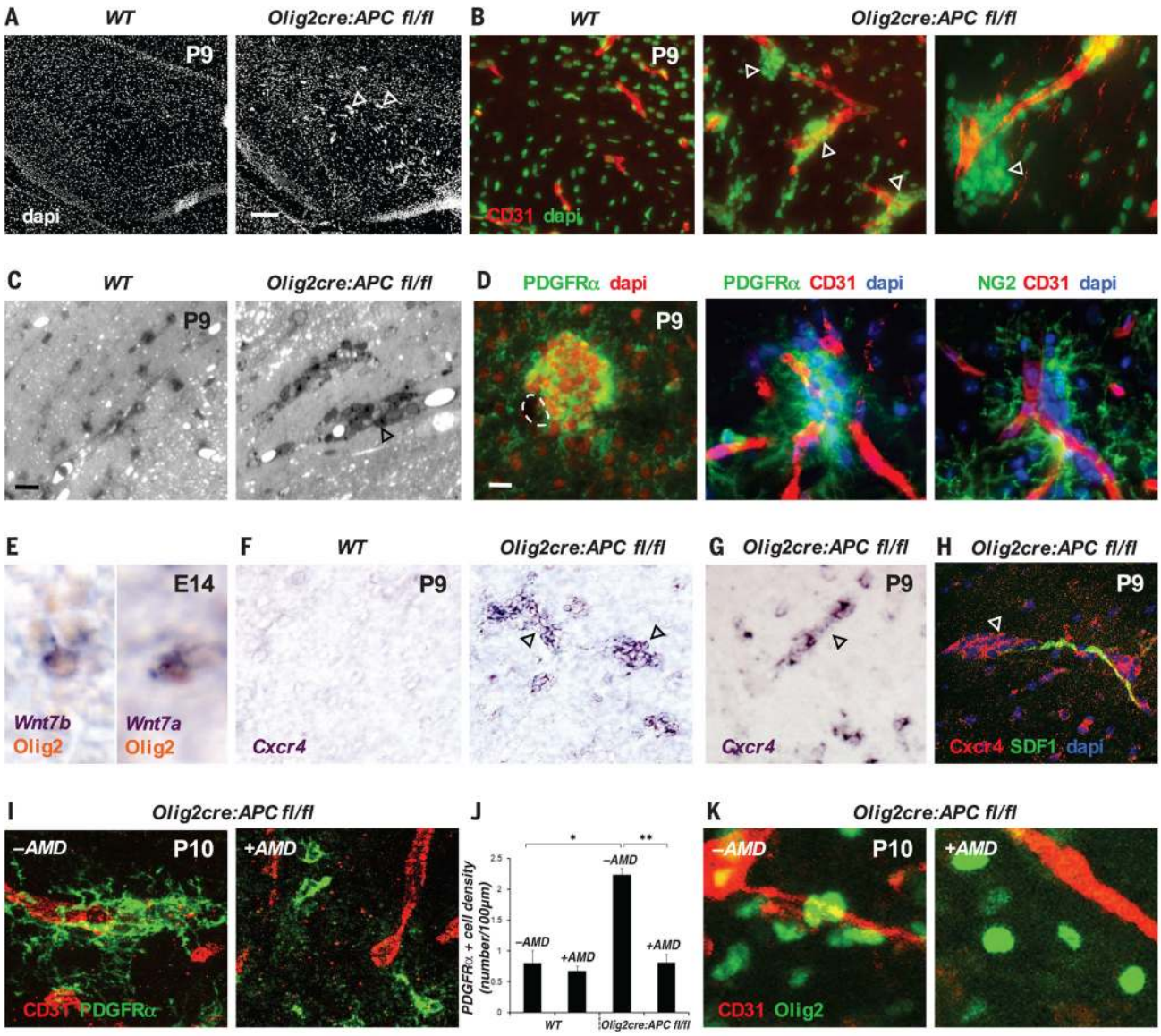

Fig. 4. A Wnt-activated, Cxcr4-dependent mechanism drives OPC attraction to the vasculature

(**A** to **D**) (A) Aberrant accumulations of cells (arrowheads) appear in the P9 corpus callosum associated with the CD31^{+} vasculature (B) of *Olig2-cre:Apc$^{flox/flox}$* mice; can be seen in resin sections stained with Toluidine blue (C); and represent OPCs, as labeled by PDGFRα and NG2 staining (D). (**E**) OPCs produce Wnt7a and Wnt7b at E14 during embryonic migration. (**F** to **H**) (F) Wnt activation in P9 *Olig2-cre:Apc$^{flox/flox}$* corpus callosum (F) or spinal cord (G) leads to marked up-regulation (compared with wild type) of *Cxcr4* mRNA [(F) and (G)] and protein (H) in clustered OPCs (arrowheads) associated with SDF1-expressing endothelium (H). (**I**) Treatment of *Olig2-cre:Apc$^{flox/flox}$* spinal cord with the Cxcr4/SDF1 inhibitor AMD3100 (+AMD) leads to a reduction in clustered OPCs associated with the vasculature, as compared with controls (−AMD). (**J**) Number of PDGFRα^{+} OPCs on a vessel in P10 spinal cord in WT versus untreated or AMD3100-treated *Olig2-cre:Apc$^{flox/flox}$* mice, expressed as number of cells on each 100-μm CD31 vessel segment

(*$P = 8.9 \times 10^{-5}$, **$P = 1.9 \times 10^{-4}$, Bonferroni test, $n = 4$ animals per group). (**K**) Treatment of P10 corpus callosum *Olig2-cre:Apc*$^{flox/flox}$ slices ex vivo overnight with 10 μg/ml of AMD3100 (+AMD, right panel) leads to a reduction in vessel-associated OPC clustering, as compared with untreated controls (−AMD, left panel). Scale bars: 120 μm (A); 10 μm [(C) and (D)].